Experimental and Molecular Pathology 145 (2026) 105029

Contents lists available at ScienceDirect

Experimental and Molecular Pathology

journal homepage: www.elsevier.com/locate/yexmp

Preliminary evidence that adipose tissue contributes to serum proprotein convertase subtilisin/kexin type 9 levels in murine models of metabolic liver injury

Sabrina Krautbauer [a,b], Florian Weber [c], Gerhard Liebisch [a], Christa Buechler [b,*]

[a] Institute of Clinical Chemistry and Laboratory Medicine, Regensburg University Hospital, 93053 Regensburg, Germany
[b] Department of Internal Medicine I, Regensburg University Hospital, 93053 Regensburg, Germany
[c] Institute of Pathology, University of Regensburg, 93053 Regensburg, Germany

ARTICLE INFO

Keywords:
High-fat diet
Fatty liver
Cholesterol
Adipose tissue

ABSTRACT

Metabolic dysfunction-associated steatotic liver disease (MASLD) is closely associated with obesity. Excess cholesterol, the hepatic and circulating levels of which are regulated by proprotein convertase subtilisin/kexin type 9 (PCSK9), exacerbates MASLD. Data on hepatic and circulating PCSK9 protein expression in MASLD are inconsistent, and PCSK9 levels in different adipose tissues have not been well studied. Here, we used two MASLD mouse models that develop hepatic steatosis, one with weight gain and one with weight loss. These models enable distinguishing between the effects of obesity and MASLD. In the high-fat diet model, hepatic PCSK9 protein was normal. PCSK9 protein was increased in the serum and epididymal fat of the mice. In mice fed a methionine-choline-deficient diet, PCSK9 protein was normal in the liver, brown fat, subcutaneous fat, epididymal, and perirenal adipose tissue. Serum PCSK9 levels were reduced, suggesting that the lower fat mass of these mice contributed to the reduction. It is noteworthy that PCSK9 expression was low in adipocytes compared to hepatocytes. In addition, stromal vascular cells residing within adipose tissue contribute to PCSK9 protein levels in adipose tissue. PCSK9 protein was similar in subcutaneous, epididymal, and perirenal adipose tissue and was lowest in brown adipose tissue, indicating a more prominent expression in white adipose tissues. The current study shows that PCSK9 is expressed in both white and brown adipose tissues, and suggests that obesity rather than liver steatosis is associated with higher serum PCSK9 levels.

1. Introduction

Proprotein convertase subtilisin/kexin type 9 (PCSK9) plays an essential role in cholesterol metabolism, and high levels of PCSK9 in the circulation result in hypercholesterolemia due to reduced low-density lipoprotein (LDL) uptake by hepatocytes (Grewal and Buechler, 2022). Blocking PCSK9 lowers serum cholesterol levels and enhances hepatic LDL uptake by increasing the expression of LDL receptors (Grewal and Buechler, 2022).

Metabolic dysfunction-associated steatotic liver disease (MASLD), formerly known as non-alcoholic fatty liver disease (NAFLD), is a common chronic liver disease. Patients with MASLD are often overweight or obese and store excess triglycerides in the liver (Buechler et al., 2011; Tilg, 2010; Yeh and Brunt, 2014). There is experimental evidence that PCSK9 has a role in the pathogenesis of MASLD. Male PCSK9−/− mice on a high-fat diet had excessive liver steatosis, inflammation, and fibrosis compared with their respective controls (Lebeau et al., 2019a). PCSK9−/− mice fed a high-fat, high-cholesterol diet accumulated free cholesterol, which is a cytotoxic metabolite, in the liver and displayed more inflammation and fibrosis than controls (Ioannou et al., 2022). Whereas these studies suggest a protective role of PCSK9, there is also evidence that PCSK9 contributes to MASLD severity. Male C57BL/6 N mice with human PCSK9 overexpression in the liver had increased plasma cholesterol and triglyceride levels, hepatic steatosis, and inflammation (Grimaudo et al., 2021). Blocking PCSK9 with alirocumab ameliorated methionine-choline-deficient (MCD) diet-

Abbreviations: ELISA, Enzyme-linked immunosorbent assay; ESI-MS/MS, electrospray ionization tandem mass spectrometry; HFD, high-fat diet; LDL, low-density lipoprotein; MASLD, Metabolic dysfunction-associated steatotic liver disease; MCD, methionine-choline-deficient; NAFLD, Non-alcoholic fatty liver disease; PCSK9, Proprotein convertase subtilisin/kexin type 9; SD, standard diet.

* Corresponding author.
E-mail address: christa.buechler@klinik.uni-regensburg.de (C. Buechler).

https://doi.org/10.1016/j.yexmp.2026.105029
Received 2 June 2025; Received in revised form 21 January 2026; Accepted 23 January 2026
Available online 28 January 2026

Table 1
Body weight, liver weight, weights of white adipose tissues, and serum insulin levels of mice fed a SD or HFD for 14 weeks.

Tissue weights and lipid levels	SD	HFD	*p*-value
Body weight, g	32 (28–38)	44 (37–48)	**
Liver weight, g	1.3 (1.1–1.7)	3.3 (1.4–4.0)	**
Subcutaneous fat, g	0.5 (0.2–0.8)	1.4 (1.2–1.6)	**
Perirenal fat, g	0.4 (0.3–0.6)	1.1 (1.0–1.1	**
Epididymal fat, g	1.0 (0.6–1.7)	1.7 (1.6–2.0)	*
Serum insulin, µg/l	0.5 (0.3–0.71)	1.1 (0.8–2.5)	**

* $p < 0.05$.
** $p < 0.01$.

induced steatohepatitis (He et al., 2021).

Clinical studies have provided evidence for the beneficial effects of PCSK9-inhibiting antibody therapies in MASLD (Scicali et al., 2021; Shafiq et al., 2020). Whether carriers of PCSK9 loss-of-function variants are protected from MASLD is less clear. This was described in one study (Grimaudo et al., 2021), whereas increased hepatic steatosis of carriers compared to non-carriers was observed by a second study (Baragetti et al., 2017). Others have reported normal liver function in PCSK9 loss-of-function carriers (Kotowski et al., 2006; Lebeau et al., 2021; Rimbert et al., 2021).

It is not yet clear whether hepatic PCSK9 levels are altered in patients with MASLD (Grewal and Buechler, 2022). Here, increased hepatic expression of PCSK9, as well as similar levels to those observed in the livers of control subjects, has been reported (Emma et al., 2020; Grimaudo et al., 2021; Theocharidou et al., 2018). Similarly, the association of blood PCSK9 levels with liver steatosis and clinical markers of liver injury is still unclear (Paquette et al., 2020; Ruscica et al., 2016; Wargny et al., 2018).

Mice fed a high-fat diet to induce liver steatosis are commonly used in MASLD research (Schattenberg and Galle, 2010), and increased PCSK9 protein was detected in the liver and in the blood of overweight mice (Lebeau et al., 2019b). Mice fed an MCD diet develop metabolic dysfunction-associated steatohepatitis (MASH) and also have higher hepatic PCSK9 expression and blood PCSK9 levels (Mijiti et al., 2024). These studies suggest that PCSK9 expression of hepatocytes, which are the major site of PCSK9 synthesis, is increased in MASLD and contributes to higher serum levels (Grewal and Buechler, 2022).

Notably, PCSK9 is also expressed in adipocytes, and PCSK9−/− mice had excess intra-abdominal fat when fed a normal or a high-fat diet (Baragetti et al., 2017; Roubtsova et al., 2011). Fat accumulation in the visceral regions of the body is associated with a high risk of developing MASLD (Buechler et al., 2011; Gordito Soler et al., 2024), showing that PCSK9 loss may have MASLD promoting activities. However, an increased fat mass of the PCSK9 null mice was not observed in the study by Lebeau et al., and here male control and PCSK9 null mice had comparable gonadal, inguinal, and brown fat mass (Lebeau et al., 2019a).

PCSK9 expressed in visceral adipose tissue was positively associated with body mass index (Bordicchia et al., 2019), and serum PCSK9 levels were increased in the obese. In obese patients following weight loss after bariatric surgery, circulating PCSK9 levels were decreased (Jamialahmadi et al., 2022; Zenti et al., 2020) whereas Ghanim et al. reported only a marginal effect of marked weight loss on plasma PCSK9 levels (Ghanim et al., 2018).

At present, the role of PCSK9 in obesity and MASLD as well as its expression in the liver and serum levels in these diseases are unclear and it is difficult to define whether it is associated with body mass index alone, with liver steatosis or both. Obese people commonly have hypercholesterolemia (Feingold, 2000) caused by disturbed cholesterol synthesis and absorption, as well as processing of lipoproteins (Mc Auley, 2020), but whether PCSK9 has a role herein is unclear. Moreover, besides the liver, adipose tissue may provide PCSK9 to the circulation

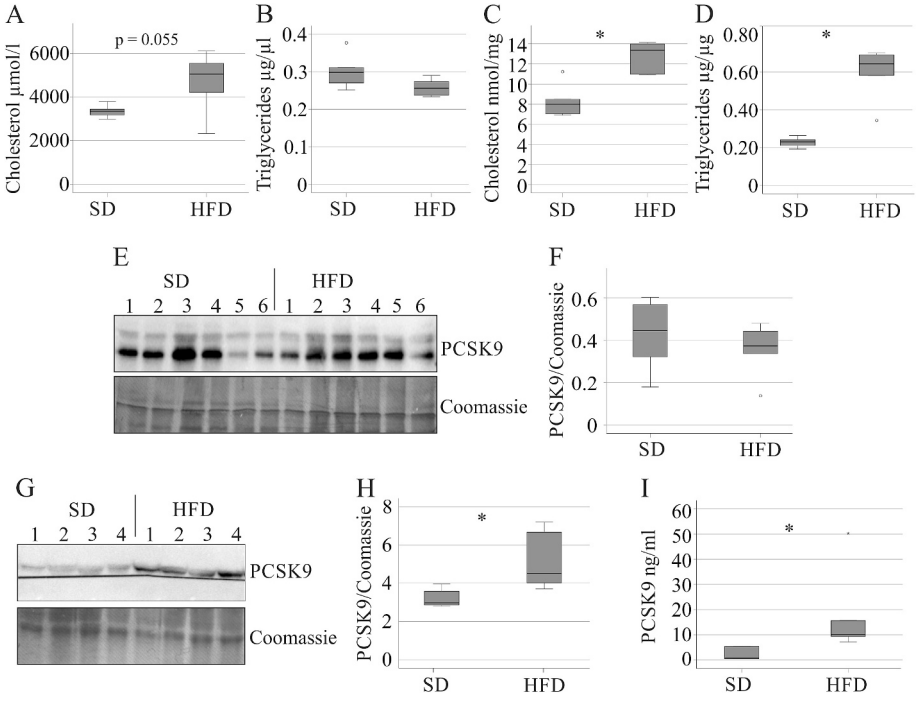

Fig. 1. Cholesterol, triglycerides, and PCSK9 in the serum and liver of mice fed a standard diet (SD) or a high-fat diet (HFD). A Cholesterol in the blood of mice fed an SD or an HFD. B Triglycerides in the blood of mice fed an SD or an HFD. The small circle in the box plot marks an outlier. C Cholesterol in the liver of mice fed an SD or an HFD. The small circle in the box plot marks an outlier. D Triglycerides in the liver of mice fed an SD or an HFD. The small circle in the box plot marks an outlier. E PCSK9 protein in the liver of 6 mice fed an SD, and 6 mice fed an HFD. Coomassie-stained membrane was used as a loading control. F PCSK9 protein in the liver of 6 mice fed an SD and 6 mice fed an HFD was quantified by ImageJ. The small circle in the box plot marks an outlier. G PCSK9 protein in the serum of 4 mice fed an SD or HFD. Coomassie-stained membrane was used as an loading control. H PCSK9 protein in serum of 5 mice each was quantified by ImageJ. I PCSK9 protein in serum of 5 mice fed an SD and 5 mice fed an HFD analysed by ELISA. The small asterisk in the box plot marks an outlier. * $p < 0.05$.

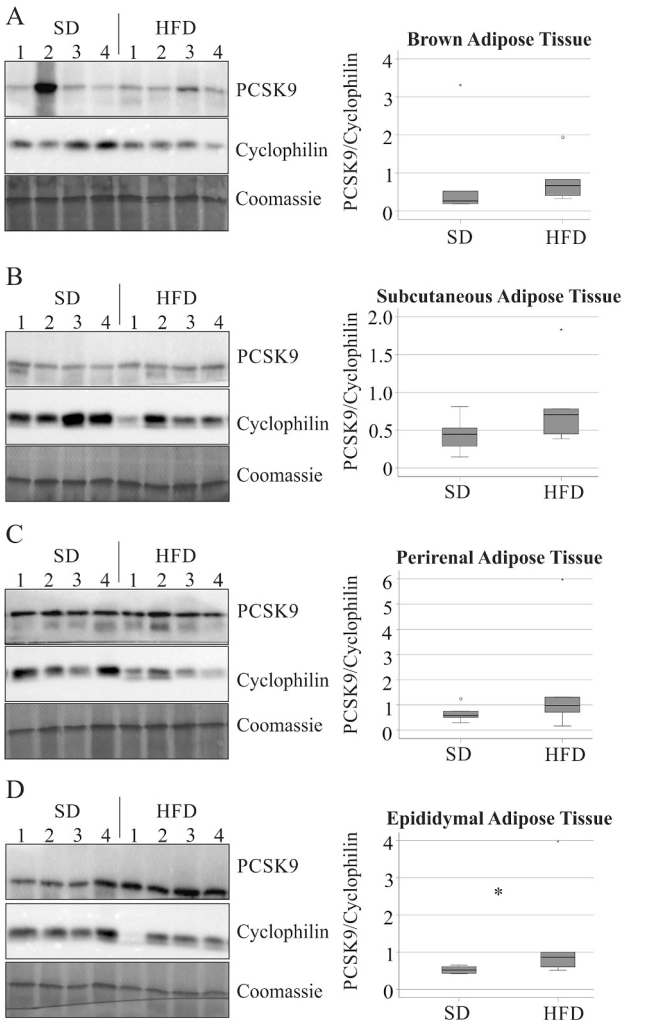

Fig. 2. PCSK9 protein in adipose tissues of mice fed a standard diet (SD) or a high-fat diet (HFD). A PCSK9 protein in brown fat, B subcutaneous fat, C perirenal fat and D *epi*didymal fat of 4 mice fed an SD and 4 mice fed an HFD, and quantification of PCSK9 protein in 6 mice each. Cyclophilin A was used as loading control. * $p < 0.05$. Small circles and asterisks in the box plots mark outliers. * $p < 0.05$.

Table 2
Body weight, liver weight, weights of white adipose tissues, and lipid levels of mice fed a control chow or MCD diet for 2 weeks.

Tissue weights and lipid levels	Control	MCD	p-value
Body weight, g	28 (25–28)	20 (17–20)	**
Liver weight, g	1.2 (1.1–1.3)	0.8 (0.6–1.2)	*
Subcutaneous fat, g	0.30 (0.20–0.37)	0.09 (0.09–0.11)	**
Perirenal fat, g	0.25 (0.15–0.35)	0.03 (0.02–0.04)	**
Epididymal fat, g	0.66 (0.56–0.83)	0.14 (0.09–0.14)	**
Liver triglycerides, mmol/g	7.3 (4.3–12.6)	30.8 (24.0–41.2)	*
Liver cholesterol, nmol/mg	6.3 (5.8–7.8)	6.4 (4.3–10.5)	
Serum cholesterol, mg/dl	116 (94–168)	73 (62–138)	

* $p < 0.05$.
** $p < 0.01$.

and contribute to hypercholesterolemia, a common comorbidity of obesity and MASLD (Feingold, 2000; Nabi et al., 2022).

There are different types of fat in the body. Brown fat produces heat, and its activation may achieve weight loss (Harb et al., 2023). Storage of triglycerides in subcutaneous fat protects other organs from steatosis and insulin resistance (Bluher, 2020; Hajer et al., 2008). Intra-abdominal fat, such as visceral fat, is associated with metabolic diseases, including type 2 diabetes and MASLD (Jensen, 2008; Schaffler et al., 2005; Wajchenberg, 2000). Gonadal and perirenal adipose tissues in mice are often used to study the role of visceral fat in metabolic diseases (Masternak et al., 2012; Mulder et al., 2016).

PCSK9 protein levels in the different fat depots of mice with MASLD have not been determined. Obesity is a risk factor for MASLD, and most patients have excess body fat (Tilg and Moschen, 2010). Therefore, it is difficult to discriminate between the effects of obesity and liver steatosis. In this study, hepatic PCSK9 protein was determined in mice fed either a high-fat diet or an MCD diet to evaluate whether hepatic steatosis is related with higher systemic PCSK9. High-fat diet leads to weight gain and MCD diet to weight loss but both models develop liver steatosis (Schattenberg and Galle, 2010). PCSK9 is detected in serum, is expressed in liver and adipose tissue (Grewal and Buechler, 2022), and in this study, PCSK9 protein expression was determined in blood, liver, subcutaneous, epididymal, perirenal, and brown adipose tissue of mice with MASLD.

2. Materials and methods

2.1. Animal experiments

Male wild type mice were obtained from The Jackson Laboratory (Bar Harbor, USA). Mice were maintained on a 12-h light/dark cycle and housed in groups of three to five animals per cage. At 14 weeks of age, animals were given either ad libitum access to a control diet (ssniff® EF acc. D12450B(I) mod., SD) or a high-fat diet (ssniff® EF R/M, D12451, 42% energy from fat, HFD) (Ssniff, Soest, Germany) for a further 14 weeks ($n = 6$ per group). Mice (14 weeks old) were also fed an MCD diet (E15653–94, Ssniff, Soest, Germany) or the respective control diet for a further two weeks (n = 6 per group). Rising concentrations of CO_2 produced loss of consciousness, which was followed by cervical dislocation. Liver, and adipose tissue, and serum were collected from overnight fasted mice. Tissues were excised, frozen in liquid nitrogen, and stored at −80 °C.

The procedures were approved by the laboratory animal committee of the University of Regensburg and complied with the German Animal Welfare Act and the guidelines for the care and use of laboratory animals of the Institute for Laboratory Animal Research, 1999. Experiments were performed in accordance with institutional and governmental regulations for the use of animals (Government of Upper Palatinate and Lower Franconia, numbers of ethics votes: 54-2532.1-30/13 and 54-2532.1-31/14).

2.2. Immunoblot

Tissues were solubilised in radioimmunoprecipitation assay lysis buffer (50 mM Tris-HCl, pH 7.4, 150 mM NaCl, 5 mM EDTA, 0.05% *v*/v Nonidet P-40, 1% v/v sodium deoxycholate, 1% v/v Triton X-100 and 0.1% v/v SDS). Twenty µg of protein was separated by SDS-PAGE and transferred to PVDF membranes (Bio-Rad Laboratories GmbH, Feldkirchen, Germany). Incubations with antibodies were performed overnight in 1% BSA in PBS, 0.1% Tween. Immunodetection was performed using the ECL Western blot detection system (Amersham Pharmacia, Deisenhofen, Germany). Antibodies against GAPDH (order number: 2118) and cyclophilin A (order number: 2175) were purchased from Cell Signaling Technologies (Leiden, Netherlands), and antibodies against PCSK9 from Bio-techne (order number: MAB3888; Wiesbaden-Nordenstadt, Germany).

2.3. Quantification of fecal fatty acids and bile acids

Mouse feces were collected in 70% isopropanol and stored at −80 °C until use. Feces samples were homogenised in a gentleMACS™ dissociator (Miltenyi Biotec GmbH, Bergisch Gladbach, Germany), and

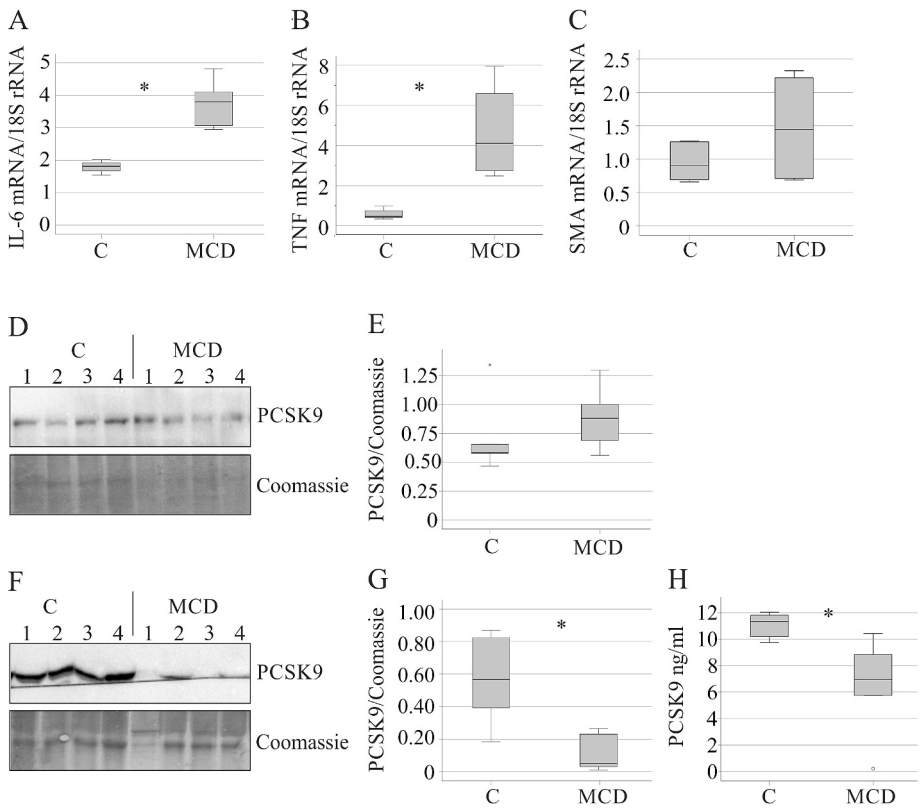

Fig. 3. PCSK9 in the serum and liver of mice fed a control or a methionine-choline deficient (MCD) diet. A *Interleukin (IL)-6* mRNA of 4 mice fed a control (C), and 5 mice fed a MCD diet. B *Tumor necrosis factor* (*TNF*) mRNA of 6 mice fed a control (C), and 4 mice fed a MCD diet. C *Alpha-smooth muscle actin* (*SMA*) mRNA of 6 mice fed a control (C), and 6 mice fed a MCD diet. D PCSK9 protein in the liver of 4 mice fed a control (C), and 4 mice fed a MCD diet. Coomassie stained membrane was used as loading control. E PCSK9 protein in the liver of 5 mice each was quantified by ImageJ. The small asterisk in the box plots marks an outlier. F PCSK9 protein in the serum of 4 mice fed a control (C), and 4 mice fed a MCD diet. Coomassie-stained membrane was used as loading control. G PCSK9 protein in the serum of 5 mice each was quantified by ImageJ. H PCSK9 protein in serum was quantified by ELISA. The small circle in the box plot marks an outlier. * $p < 0.05$.

prepared for analysis as described for human fecal samples (Schott et al., 2018).

Concentrations of total fecal fatty acids were determined by gas chromatography coupled to mass spectrometry as described previously (Ecker et al., 2012) with some modifications. Homogenates were derivatized to fatty acid methyl ester. The initial column temperature of 50 °C was held for 0.75 min, increased with 40 °C/min to 110 °C, with 6 °C/min to 210 °C, with 15 °C/min to 250 °C and held for 2 min. Iso- and anteiso- fatty acid methyl ester standards were applied to identify branched chain fatty acids and to calibrate the instrument response.

Fecal bile acids were quantified by liquid chromatography-tandem mass spectrometry using a modified method for serum with stable isotope dilution analysis (Krautbauer et al., 2016; Scherer et al., 2009).

2.4. Analysis of serum and liver lipids

Triglyceride concentrations were measured using the GPO-PAP micro-test (purchased from Roche, Mannheim, Germany). Serum cholesterol was analysed with an assay from Diaglobal (Berlin, Germany) or electrospray ionization tandem mass spectrometry (ESI-MS/MS) (Liebisch et al., 2006). Lipids quantification in liver tissues by direct flow injection ESI–MS/MS was done in positive ion mode as described (Liebisch et al., 2004). Briefly, samples were prepared according to the method by Bligh and Dyer (1959), and non-naturally occurring lipid species were added as internal standards. Analysis was performed on a Quattro Ultima triple-quadrupole mass spectrometer (Micromass, Manchester, UK) equipped with an autosampler (HTS PAL, Zwingen, Switzerland) and a binary pump (Model 1100, Agilent, Waldbronn, Germany). Free cholesterol and cholesteryl ester levels were measured using a fragment ion of *m/z* 369 (Liebisch et al., 2006). Liver lipids are expressed as nmol/mg wet weight (Haberl et al., 2021; Horing et al., 2021).

2.5. Cell culture

The 3 T3-L1 preadipocytes were from the American Type Culture Collection (Manassas, VA, USA). Cells were cultured at 37 °C in 5% CO_2 in Dulbecco's modified Eagle's medium (Biochrom, Berlin, Germany) supplemented with 10% neonatal calf serum (Sigma Bioscience, Deisenhofen, Germany) and 1% penicillin/streptomycin (PAN, Aidenbach, Germany). For adipogenesis, 3 T3-L1 preadipocytes were grown to confluence and differentiated into adipocytes as described (Bauer et al., 2011).

2.6. Semiquantitative real-time PCR

Semiquantitative real-time PCR used the LightCycler® FastStart DNA Master SYBR Green I Kit from Roche (Mannheim, Germany) as described (Bauer et al., 2011). Primers were 5′ttc cat cca gtt gcc ttc tt 3′and 5′ttc tgc aag tgc atc atc gt 3′ to analyse IL-6, 5′ccg atg ggt tgt acc ttg tc 3′ and 5′ggg ctg ggt aga gaa tgg at 3′ to analyse TNF, 5′ cca gca cca tga aga tca ag 3′and 5′ ctt cgt cgt att cct gtt tgc 3′for alpha-smooth muscle actin, and 5′gat tga tag ctc ttt ctc gat tcc 3′and 5′cat cta agg gca tca cag acc 3′ to analyse 18S rRNA. Expression of PCSK9 and GAPDH was determined using the LightCycler 480 from Roche. PrimePCR™ PreAmp for SYBR® Green Assay: Pcsk9, Mouse and PrimePCR™ PreAmp for SYBR® Green Assay: GAPDH, Mouse (BioRad, Hercules, CA, USA) were used for amplification.

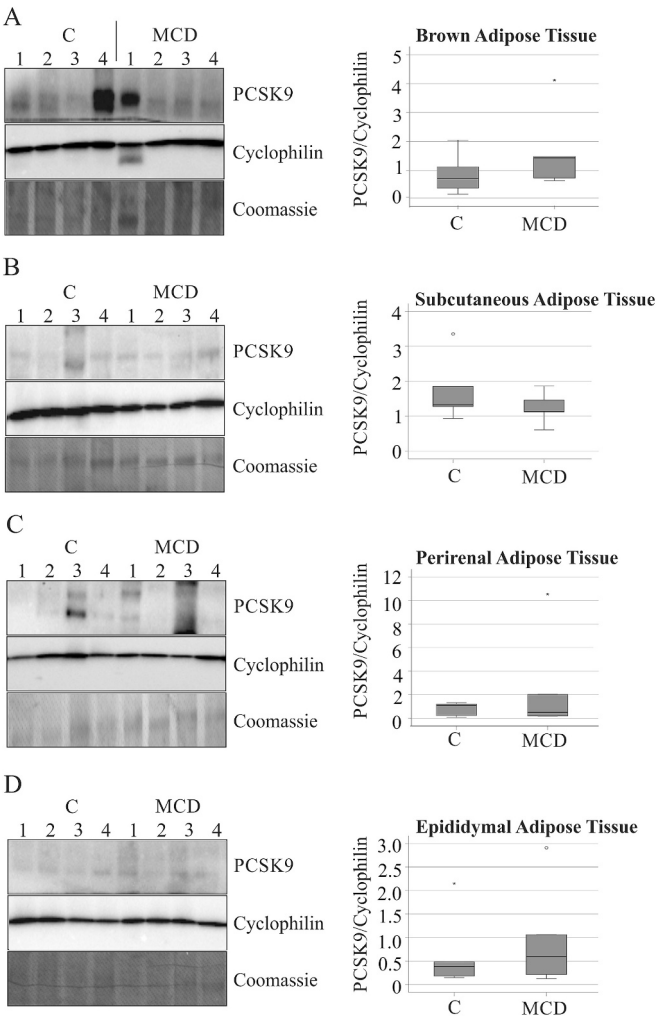

Fig. 4. PCSK9 in adipose tissues of mice fed a control or a methionine-choline deficient (MCD) diet. A PCSK9 protein in brown fat, B subcutaneous fat, C perirenal fat and D epididymal fat of 4 mice fed a control (C) and 4 mice fed a MCD diet, and quantification of PCSK9 protein in 5 mice each. Cyclophilin A was used as loading control. Small circles and asterisks in the box plots mark outliers.

2.7. Sirius Red staining, immunohistochemistry of PCSK9, and insulin and PCSK9 ELISA

Formalin-fixed liver tissues were embedded in paraffin. Slices were cut into 3 μm sections and stained with Sirius Red. Immunohistochemistry of human adipose tissue was performed as described (Weber et al., 2023) using a monoclonal human PCSK9 antibody from ThermoFisher (order number: MA5–32843, Waltham, MA, USA). Immunohistochemistry to detect alpha-smooth muscle actin in murine liver used the antibody from Abcam (order number: ab7817, Cambridge, UK; dilution 1:75). The protocol for this method has been described (Rein-Fischboeck et al., 2017). Insulin ELISA was from Mercodia (order number: 10-1247-10, Uppsala, Sweden). ELISA for murine PCSK9 analysis was from Biotechne (order number: MPC900).

2.8. Statistics

Data are shown as box plots, with small circles and asterisks indicating outliers. Mild outliers (between 1.5 and 3 interquartile ranges from the box) are denoted by circles, while extreme outliers (beyond 3 interquartile ranges from the box) are signified by asterisks. Mann-Whitney *U* test, Kruskal-Wallis test and Student's *t*-test were used as statistical tests (SPSS 26; IBM Corp., Armonk, NY, USA, released 2019). Data in tables are presented as median, minimum and maximum values. A value of $p < 0.05$ was considered significant.

3. Results

3.1. PCSK9 protein in the liver, adipose tissues, and serum of mice fed a high-fat diet

The expression of hepatic and serum PCSK9 protein in MASLD is still unresolved (Grewal and Buechler, 2022). Adipose tissue has a crucial role in MASLD (Adolph et al., 2017), but PCSK9 levels in fat have been hardly studied. Therefore, PCSK9 protein levels were analysed in adipose tissues and the liver of mice fed a standard diet (SD) or a high-fat diet (HFD). Tissues and serum were obtained of mice, which were fasted overnight. These latter mice had higher body weight, liver weight, and subcutaneous, perirenal, and epididymal fat mass (Table 1). Serum insulin of mice fed a HFD was increased (Table 1).

Mice fed the HFD had higher cholesterol in the blood in the fasted state ($p = 0.055$; Fig. 1A). Serum triglycerides of the SD and HFD-fed mice were similar between the groups (Fig. 1B). Liver cholesterol and triglycerides of the mice were significantly increased (Fig. 1C, D).

Cholesterol can be converted to bile acids for fecal excretion (Calzadilla et al., 2022). The primary bile acid chenodeoxycholic acid and the secondary bile acid deoxycholic acid did not change in the feces of HFD-fed mice (Fig. S1A, B). The levels of fecal ursodeoxycholic acid strongly declined (Fig. S1C).

Mice fed a HFD had increased levels of serum insulin (Table 1) and fecal fatty acids (Fig. S1D).

PCSK9 in the liver, which was analysed by immunoblot in tissues of 6 SD and 6 HFD-fed mice (Fig. 1E, F) and by ELISA in tissues of 4 animals each where levels were 73 (35–87) pg PCSK9/mg protein for SD and 183 (49–498) pg PCSK9/mg protein for HFD ($p = 0.122$), were similar. PCSK9 mRNA was significantly increased in the liver of the HFD-fed mice. Expression was 3.1 (0.8–6.7) for 6 SD and 12.8 (6.0–25.6) for 6 HFD-fed mice ($p = 0.006$). Serum PCSK9 levels, which were analysed in 5 animals/group either by immunoblot or ELISA, were increased in the high-fat diet fed mice (Fig. 1G, H, I).

It was also analysed whether PCSK9 levels change in mice under fed conditions. These mice were fed an SD or HFD diet for 14 weeks, and the study protocol was identical to that of the animals described in Table 1. Body weight, liver weight ($p = 0.055$), and adipose tissue weights were increased upon HFD feeding (Table S1). Here, serum and liver tissues were obtained from overnight fasted mice as well as mice with access to food.

Mice fed the HFD had higher cholesterol in the blood in the fasted and fed state (Fig. S2 A). This difference was significant for the mice in the fasted situation (Fig. S2 A). Triglycerides increased in the fed compared to the fasted state of SD fed mice. This effect was blunted in the HFD-fed animals in accordance with previous studies (Uchida et al., 2012) (Fig. S2B). Otherwise, blood triglyceride levels were similar between the groups (Fig. S2B).

Serum PCSK9 levels of the HFD-fed mice in the fed state were significantly increased, and there was a similar trend in the fasted mice ($p = 0.071$) (Fig. S2C).

PCSK9 protein was also analysed by immunoblot in brown fat, subcutaneous, perirenal, and epididymal adipose tissues of 6 mice fed an SD and 6 mice fed an HFD. PCSK9 protein was higher in the epididymal fat depot of HFD-fed mice, and did not differ from the controls in the other fat depots (Fig. 2A - D). PCSK9 protein analysed by ELISA in epididymal fat of 5 mice fed the SD, and 6 mice fed the HFD was 1.0 (0.2–1.2) ng PCSK9/mg total protein and 1.8 (1.0–3.3) ng PCSK9/mg total protein, respectively ($p = 0.018$). There was no significant difference in PCSK9 levels in brown fat ($p = 0.127$) in accordance with immunoblot data (Fig. 2A).

PCSK9 mRNA in epididymal fat of 3 SD fed mice was 1.6 (1.6–1.8)

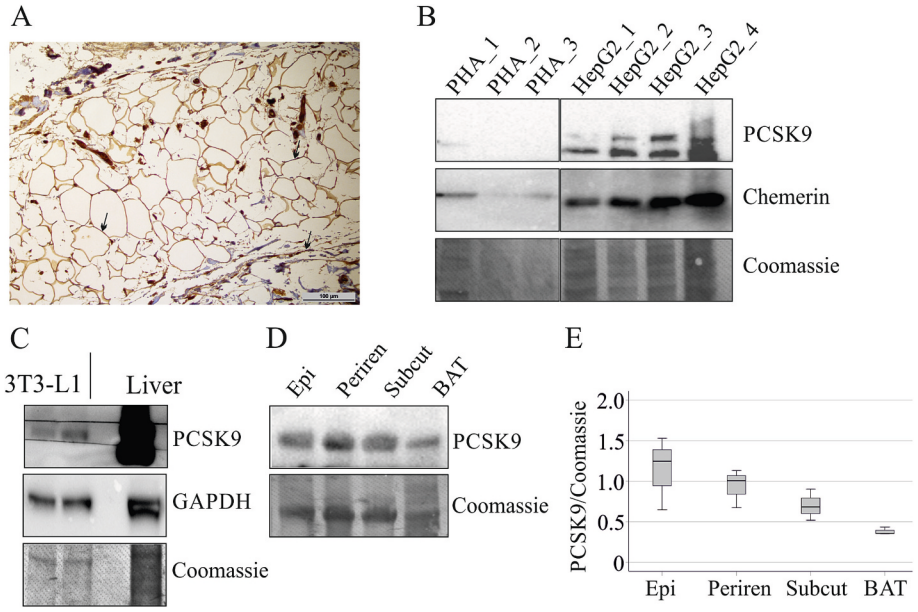

Fig. 5. PCSK9 in adipocytes and adipose tissues. A Immunohistochemistry of PCSK9 protein in human adipose tissue (black arrows point to endothelial cells and adipocytes expressing PCSK9). B PCSK9 protein of primary human adipocytes (PHA) and HepG2 cells. The samples were analysed on the same membrane, which was cut to remove data not relevant for this analysis. C PCSK9 protein of 3 T3-L1 adipocytes compared to PCSK9 in the murine liver. Coomassie-stained membrane and GAPDH were used as loading controls. D PCSK9 protein in epididymal fat (epi), perirenal fat (periren), subcutaneous fat (subcut), and brown fat (BAT) of mice. E Quantification of PCSK9 in the different fat depots of 3 mice. Coomassie-stained membrane was used as loading control.

and was 1.2 (0.5–4.5) in 6 HFD-fed animals and did not differ between the groups ($p = 0.439$).

PCSK9 protein in the liver, adipose tissue, and serum of mice fed a methionine-choline deficient diet.

The MCD diet induces metabolic dysfunction-associated steatohepatitis (MASH) in mice and lowers body weight and fat mass (Schattenberg and Galle, 2010) (Table 2).

The mice developed liver inflammation as assessed by higher expression of *interleukin-6* and *tumor necrosis factor* mRNA (Fig. 3A, B and (Rein-Fischboeck et al., 2019)). The expression of *alpha-smooth muscle actin* of mice fed the control and MCD diet was similar (Fig. 3C and (Rein-Fischboeck et al., 2019)). Alpha-smooth muscle actin immunostaining could not detect this protein in the liver of control and MCD animals (Fig. S3A, B). Sirius Red staining showed that fibrosis did not develop in the mice fed the MCD chow for 2 weeks (Fig. S3C,D).

The hepatic cholesterol concentration and serum cholesterol levels did not significantly change (Table 2 and (Rein-Fischboeck et al., 2019)). Liver triglycerides of mice fed the MCD diet were significantly increased (Table 2 and (Rein-Fischboeck et al., 2019). PCSK9 protein levels in the liver of both groups were similar (Fig. 3D, E). PCSK9 analysed by ELISA in the liver of 5 mice fed the control diet and 5 mice fed the MCD diet was 90 (40–120) pg PCSK9/mg total protein and 110 (40–180) pg PCSK9/mg total protein, respectively ($p = 0.347$).

Serum PCSK9 levels of mice with MASH were significantly reduced, as shown by immunoblot and by ELISA (Fig. 3F-H). PCSK9 mRNA in the liver of 6 control fed mice was 99 (43–194) and 23 (4–131) in the liver of 6 MCD diet fed animals, and was similar between the groups ($p = 0.078$).

The expression of PCSK9 in the fat depots of different mice showed a high variability in brown fat and perirenal adipose tissue. Expression of PCSK9 in the different adipose tissues did not decline in the MCD diet fed mice (Fig. 4A-D). PCSK9 mRNA in epididymal fat of 5 control fed mice was 9.8 (0.7–73.5) and 3.8 (1.9–7.3) in 5 MCD fed mice and did not differ between the groups ($p = 0.117$).

3.2. PCSK9 protein in adipocytes

Though it is known for a long time that PCSK9 is expressed in adipose tissue (Grewal and Buechler, 2022), this has not been analysed in depth. Immunohistochemistry of human adipose tissue revealed expression of PCSK9 protein by adipocytes and endothelial cells of the blood vessels (Fig. 5A). Immunoblot of protein isolated from primary human adipocytes of three different donors, and HepG2 cells (4 different batches) could hardly detect PCSK9 protein in the fat cells. HepG2 cells expressed PCSK9 protein as expected (Thorlacius-Ussing et al., 2016). Chemerin, a protein known to be expressed by adipocytes and hepatocytes (Spirk et al., 2020; Wanninger et al., 2012), could be detected in all cell lysates (Fig. 5B). The murine 3 T3-L1 cell line can be differentiated to mature adipocytes and is used as an in-vitro model (Takahashi et al., 2008; Temple et al., 2007). In agreement with data from human cells, the expression of PCSK9 protein in these cells was low (Fig. 5C).

Analysis of different murine fat tissues could easily detect the PCSK9 protein (Fig. 5D), indicating that PCSK9 is expressed in adipocytes and stromal vascular cells, such as preadipocytes and/or blood vessels. Comparison of epididymal, perirenal, subcutaneous, and brown fat of three different mice showed the lowest expression of PCSK9 in brown fat, whereas levels in the other three fat depots were similar ($p = 0.063$; Fig. 5D, E).

4. Discussion

This is, to our knowledge, the first study to investigate the expression of PCSK9 protein in serum, the liver, and adipose tissues in murine MASLD. The analyses provide preliminary evidence suggesting that adipose tissue may contribute to PCSK9 levels in the blood.

PCSK9 has a central role in the regulation of blood cholesterol levels (Grewal and Buechler, 2022) and thus is of clinical relevance. Hypercholesterolemia is common in patients with MASLD (Nabi et al., 2022), and higher serum PCSK9 levels described in MASLD may be associated with this comorbidity (Emma et al., 2020; Ruscica et al., 2016). Obesity is a risk factor for MASLD occurrence and progression (Cusi, 2012; Marengo et al., 2015; Younossi et al., 2018), but adipose tissue expression of PCSK9 in experimental MASLD has not been determined to our knowledge.

Mice fed an HFD had increased weight of all white fat depots and the

liver. These animals stored excess triglycerides and cholesterol in the liver. Bile acids are essential for cholesterol excretion, but fecal levels of chenodeoxycholic acid and deoxycholic acid were normal. Another study also observed normal chenodeoxycholic acid but an increase of deoxycholic acid in the feces of high-fat diet fed mice (Xu et al., 2023). Fecal levels of the secondary bile acid ursodeoxycholic acid of mice fed the high-fat diet were low in accordance with previous observations (Stenman et al., 2012; Xu et al., 2023). Fecal fatty acids of the obese mice were markedly increased, as has been shown before (Zeng et al., 2022).

Hepatic PCSK9 protein levels of SD and HFD-fed mice were comparable, and were increased in serum and epididymal fat of these animals. Serum cholesterol levels of the HFD-fed mice were higher in accordance with increased serum PCSK9 levels. *PCSK9* mRNA expression in the liver of HFD-fed mice was almost 4-fold increased in comparison to SD-fed animals. Higher systemic PCSK9 protein levels and PCSK9 mRNA levels in the liver have been described in patients with liver steatosis (Grimaudo et al., 2021; Paquette et al., 2020; Ruscica et al., 2016).

This suggests higher PCSK9 protein synthesis and release into the blood in murine and human liver steatosis. However, Wargny et al. did not detect higher levels of PCSK9 in the blood of patients with MASLD. This study also showed that hepatic *PCSK9* mRNA levels did not correlate with MASH histological severity (Wargny et al., 2018). Increased PCSK9 mRNA expression in MASH, a decline of PCSK9 protein during the progression of MASLD and normal serum PCSK9 levels have also been reported (Castellano-Castillo et al., 2024). Thus, the association of PCSK9 in the blood and the liver with MASLD is still unresolved, and obesity may be a confounding factor.

Mice fed an HFD have increased fat mass and higher levels of PCSK9 protein in their epididymal fat, suggesting that adipose tissue contributes to the systemic levels of PCSK9 in obesity. Consistent with this hypothesis, six months after undergoing bariatric surgery, patients had lost a significant amount of adipose tissue, and their plasma PCSK9 levels had decreased considerably (Zenti et al., 2020). However, higher levels of PCSK9 protein in the epididymal fat of mice fed an HFD were not associated with changes in PCSK9 mRNA levels. Typically, a higher level of PCSK9 protein is the result of more PCSK9 mRNA. Processes affecting the stability of the mRNA, its translation into protein, or the fate of the protein may be altered (Xia et al., 2021). However, higher levels of PCSK9 protein in tissue may also be caused by increased uptake of PCSK9 from the bloodstream (Grewal and Buechler, 2022), or may reflect changes in the cellular composition of obese fat tissue (Sarvari et al., 2021). Serum PCSK9 levels of patients with liver cirrhosis decline, and the severity of the underlying liver disease is a confounding factor for studies analysing serum PCSK9 in MASLD (Feder et al., 2021).

The murine MCD model is characterized by massive storage of triglycerides in the liver and hepatic inflammation (Schattenberg and Galle, 2010). Cholesterol levels in the liver and serum cholesterol of the mice with MASH were normal. These animals had hepatic inflammation, as assessed by higher expression of *interleukin-6* and *tumor necrosis factor*. There were no signs of liver fibrosis, and two weeks of feeding may not be sufficient for the development of liver fibrosis. Feeding animals an MCD diet is related to massive loss of body fat mass, and the mice lost about 80% of their white fat depots. Serum PCSK9 levels were markedly declined at the end of the study. Hepatic and adipose tissue protein levels of PCSK9 as well as hepatic and epididymal PCSK9 mRNA expression of the MCD fed mice did not significantly change, suggesting that reduced fat mass is related to lower systemic PCSK9 levels.

Serum and liver PCSK9 protein in MCD-diet fed mice have been analysed before. Mice fed the MCD diet developed marked steatohepatitis and had increased hepatic PCSK9 expression and PCSK9 in blood (Mijiti et al., 2024). These animals lost about 60% of their body weight during the 6-week MCD feeding (Mijiti et al., 2024). The findings of our current study, where mice were fed the MCD diet for only 2 weeks and previous study, where mice were fed the MCD diet for 6 weeks (Mijiti et al., 2024) are not concordant with so far unknown reasons.

The mechanisms causing liver steatosis in HFD and MCD diet are different. In the HFD model, excess dietary fat induces steatosis, whereas in the MCD model, a lack of choline impairs hepatic lipid release (Schattenberg and Galle, 2010). Although sterol regulatory element-binding protein 2, the major transcription factor of PCSK9 expression, is induced in both models, upregulation of PCSK9 mRNA was only detected in the HFD model (Deng et al., 2017; Grewal and Buechler, 2022; Hu et al., 2020). The present study shows that hepatic steatosis alone is not a relevant trigger for higher PCSK9 serum levels in MASLD and that the underlying mechanisms are largely unknown. Therapies with PCSK9 blocking antibodies may not be efficient in improving MASLD (Al Hashmi et al., 2024), and the results of clinical studies are currently inconsistent (Giglio et al., 2023). The present analysis suggests that excess adipose tissue contributes to serum PCSK9 levels, emphasising the need for therapies that lower fat (Al Hashmi et al., 2024).

It should be noted that the liver weight of the MCD-diet fed mice was reduced by about 35%, and lower liver mass may also contribute to lower serum PCSK9 levels of these mice. In the high-fat diet model, liver weight was increased by 250%, and this is mostly because of the excessive storage of lipids in the liver which will not contribute to higher PCSK9 levels.

In healthy humans, fasting for up to 12 h did not alter plasma PCSK9 levels (Browning and Horton, 2010; Brugger et al., 1997), and in our mice, there were no significant differences in the systemic PCSK9 levels of fed and fasted mice. However, prolonged fasting has been associated with a decline in plasma PCSK9 levels (Browning and Horton, 2010).

The hepatocyte-specific PCSK9 knockout revealed that, in the liver, PCSK9 is exclusively expressed in hepatocytes and that the circulating PCSK9 is >95% from hepatic origin (Zaid et al., 2008). In the meantime it has been shown that hepatic stellate cells (Luquero et al., 2022) and endothelial cells also express PCSK9, which is induced in endothelial cells by high glucose (Gao et al., 2024). Moreover, the present study provided preliminary evidence that adipose tissue may contribute to circulating PCSK9 levels.

This study showed that PCSK9 protein was similarly expressed in all of the white fat depots analysed. In brown adipose tissue, PCSK9 protein levels were the lowest in comparison to the white fat depots. White and brown fat differ in many aspects, including triglyceride storage, number of mitochondria, localization in the body, and their secretomes (Hachemi and Mueez U-Din, 2023). Of the white fat depots, subcutaneous fat expansion is regarded as protective, whereas excess intra-abdominal fat is linked with metabolic diseases and MASLD (Adolph et al., 2017; Buechler et al., 2011; Farrell et al., 2012). Despite the different physiological functions of the fat tissues, PCSK9 levels in all of the adipose tissues was comparable. PCSK9 expression in 3 T3-L1 adipocytes and primary human adipocytes was rather low, and the PCSK9 protein of stromal vascular cells, which are composed of endothelial precursor cells, mesenchymal stem cells, T cells, macrophages, and preadipocytes (Nguyen et al., 2016), contributes to the PCSK9 protein level detected in whole adipose tissue. Immunohistochemistry also showed high expression of PCSK9 in blood vessel endothelial cells.

A limitation of this experimental study is that it does not provide conclusive evidence that PCSK9 levels are derived from the different adipose tissues. Despite normal hepatic PCSK9 protein expression, the levels released by the liver can be higher in MASLD.

In summary, this analysis is the first to study the PCSK9 protein in different fat depots of mice. This analysis shows that the PCSK9 protein is present in both brown and white adipose tissues. Further study is needed to determine whether higher PCSK9 expression in epididymal fat contributes to elevated PCSK9 serum levels in obesity.

CRediT authorship contribution statement

Sabrina Krautbauer: Writing – review & editing, Investigation, Conceptualization. **Florian Weber:** Writing – review & editing, Investigation. **Gerhard Liebisch:** Writing – review & editing, Formal

analysis. **Christa Buechler:** Writing – review & editing, Writing – original draft, Formal analysis, Conceptualization.

Institutional review board statement

The procedures were approved by the laboratory animal committee of the University of Regensburg and complied with the German Animal Welfare Act and the guidelines for the care and use of laboratory animals of the Institute for Laboratory Animal Research, 1999. Experiments were performed in accordance with institutional and governmental regulations for the use of animals (Government of Upper Palatinate and Lower Franconia, number of ethics votes: 54-2532.1-30/13 and 54-2532.1-31/14).

Declaration of generative AI and AI-assisted technologies in the writing process

During the preparation of this work, the author(s) used DeepL Write in order to correct typing and grammatical errors. After using this tool, the authors reviewed and edited the content as needed and take full responsibility for the content of the published article.

Funding

This research did not receive any specific grant from funding agencies in the public, commercial, or not-for-profit sectors.

Declaration of competing interest

The authors declare that they have no known competing financial interests or personal relationships that could have appeared to influence the work reported in this paper.

Acknowledgment

We are very grateful to Elena Underberg and Heidi Gschwendtner for their excellent technical assistance. We are also grateful to Dr. Lisa Rein-Fischboeck and Dr. Kristina Eisinger for preparing the mouse tissues.

Appendix A. Supplementary data

Supplementary data to this article can be found online at https://doi.org/10.1016/j.yexmp.2026.105029.

Data availability

The data are included in the manuscript. Original data and immunoblots can be obtained from the corresponding author upon reasonable request.

References

Adolph, T.E., et al., 2017. Adipokines and non-alcoholic fatty liver disease: multiple interactions. Int. J. Mol. Sci. 18. https://doi.org/10.3390/ijms18081649.

Al Hashmi, K., et al., 2024. Metabolic dysfunction-associated fatty liver disease: current therapeutic strategies. Front. Nutr. 11, 1355732. https://doi.org/10.3389/fnut.2024.1355732.

Baragetti, A., et al., 2017. PCSK9 deficiency results in increased ectopic fat accumulation in experimental models and in humans. Eur. J. Prev. Cardiol. 24, 1870–1877. https://doi.org/10.1177/2047487317724342.

Bauer, S., et al., 2011. Sterol regulatory element-binding protein 2 (SREBP2) activation after excess triglyceride storage induces Chemerin in hypertrophic adipocytes. Endocrinology 152, 26–35. https://doi.org/10.1210/en.2010-1157.

Bligh, E.G., Dyer, W.J., 1959. A rapid method of total lipid extraction and purification. Can. J. Biochem. Physiol. 37, 911–917. https://doi.org/10.1139/o59-099.

Bluher, M., 2020. Metabolically healthy obesity. Endocr. Rev. 41. https://doi.org/10.1210/endrev/bnaa004.

Bordicchia, M., et al., 2019. PCSK9 is expressed in human visceral adipose tissue and regulated by insulin and cardiac natriuretic peptides. Int. J. Mol. Sci. 20. https://doi.org/10.3390/ijms20020245.

Browning, J.D., Horton, J.D., 2010. Fasting reduces plasma proprotein convertase, subtilisin/kexin type 9 and cholesterol biosynthesis in humans. J. Lipid Res. 51, 3359–3363. https://doi.org/10.1194/jlr.P009860.

Brugger, B., et al., 1997. Quantitative analysis of biological membrane lipids at the low picomole level by nano-electrospray ionization tandem mass spectrometry. Proc. Natl. Acad. Sci. U. S. A. 94, 2339–2344. https://doi.org/10.1073/pnas.94.6.2339.

Buechler, C., et al., 2011. Adiponectin, a key adipokine in obesity related liver diseases. World J. Gastroenterol. 17, 2801–2811. https://doi.org/10.3748/wjg.v17.i23.2801.

Calzadilla, N., et al., 2022. Bile acids as inflammatory mediators and modulators of intestinal permeability. Front. Immunol. 13, 1021924. https://doi.org/10.3389/fimmu.2022.1021924.

Castellano-Castillo, D., et al., 2024. The role of PCSK9 in metabolic dysfunction-associated steatotic liver disease and its impact on bariatric surgery outcomes. Surg. Obes. Relat. Dis. 20, 652–659. https://doi.org/10.1016/j.soard.2024.01.017.

Cusi, K., 2012. Role of obesity and lipotoxicity in the development of nonalcoholic steatohepatitis: pathophysiology and clinical implications. Gastroenterology 142 (711–725), e6. https://doi.org/10.1053/j.gastro.2012.02.003.

Deng, X., et al., 2017. Regulation of SREBP-2 intracellular trafficking improves impaired autophagic flux and alleviates endoplasmic reticulum stress in NAFLD. Biochim. Biophys. Acta Mol. Cell Biol. Lipids 1862, 337–350. https://doi.org/10.1016/j.bbalip.2016.12.007.

Ecker, J., et al., 2012. A rapid GC-MS method for quantification of positional and geometric isomers of fatty acid methyl esters. J. Chromatogr. B Analyt. Technol. Biomed. Life Sci. 897, 98–104. https://doi.org/10.1016/j.jchromb.2012.04.015.

Emma, M.R., et al., 2020. Hepatic and circulating levels of PCSK9 in morbidly obese patients: relation with severity of liver steatosis. Biochim. Biophys. Acta Mol. Cell Biol. Lipids 1865, 158792. https://doi.org/10.1016/j.bbalip.2020.158792.

Farrell, G.C., et al., 2012. NASH is an inflammatory disorder: pathogenic, prognostic and therapeutic implications. Gut Liver 6, 149–171. https://doi.org/10.5009/gnl.2012.6.2.149.

Feder, S., et al., 2021. Proprotein convertase subtilisin/kexin type 9 (PCSK9) levels are not associated with severity of liver disease and are inversely related to cholesterol in a cohort of thirty eight patients with liver cirrhosis. Lipids Health Dis. 20. https://doi.org/10.1186/s12944-021-01431-x.

Feingold, K.R., 2000. In: Feingold, K.R., Adler, R.A., Ahmed, S.F., et al. (Eds.), Obesity and Dyslipidemia. [Updated 2023 Jun 19]. MDText.com, Inc, South Dartmouth (MA). Endotext [Internet]. Available from: https://www.ncbi.nlm.nih.gov/books/NBK305895/.

Gao, J.J., et al., 2024. Increase of PCSK9 expression in diabetes promotes VEGFR2 ubiquitination to inhibit endothelial function and skin wound healing. Sci. China Life Sci. 67, 2635–2649. https://doi.org/10.1007/s11427-023-2688-8.

Ghanim, H., et al., 2018. Effect of restricted caloric intake and bariatric surgery on PCSK9 concentrations in plasma. Diabetes 67. https://doi.org/10.2337/db18-2093-P.

Giglio, R.V., et al., 2023. Treatment with proprotein convertase subtilisin/kexin type 9 inhibitors (PCSK9i): current evidence for expanding the paradigm? J. Cardiovasc. Pharmacol. Ther. 28, 10742484231186855. https://doi.org/10.1177/10742484231186855.

Gordito Soler, M., et al., 2024. Usefulness of body fat and visceral fat determined by bioimpedanciometry versus body mass index and waist circumference in predicting elevated values of different risk scales for non-alcoholic fatty liver disease. Nutrients 16. https://doi.org/10.3390/nu16132160.

Grewal, T., Buechler, C., 2022. Emerging insights on the diverse roles of proprotein convertase subtilisin/kexin type 9 (PCSK9) in chronic liver diseases: cholesterol metabolism and beyond. Int. J. Mol. Sci. 23. https://doi.org/10.3390/ijms23031070.

Grimaudo, S., et al., 2021. PCSK9 rs11591147 R46L loss-of-function variant protects against liver damage in individuals with NAFLD. Liver Int. 41, 321–332. https://doi.org/10.1111/liv.14711.

Haberl, E.M., et al., 2021. Liver lipids of patients with hepatitis B and C and associated hepatocellular carcinoma. Int. J. Mol. Sci. 22. https://doi.org/10.3390/ijms22105297.

Hachemi, I., Mueez U-Din, 2023. Brown adipose tissue: activation and metabolism in humans. Endocrinol. Metab. (Seoul) 38, 214–222. https://doi.org/10.3803/EnM.2023.1659.

Hajer, G.R., et al., 2008. Adipose tissue dysfunction in obesity, diabetes, and vascular diseases. Eur. Heart J. 29, 2959–2971.

Harb, E., et al., 2023. Brown adipose tissue and regulation of human body weight. Diabetes Metab. Res. Rev. 39, e3594. https://doi.org/10.1002/dmrr.3594.

He, Y., et al., 2021. Neutrophil-to-hepatocyte communication via LDLR-dependent miR-223-enriched extracellular vesicle transfer ameliorates nonalcoholic steatohepatitis. J. Clin. Invest. 131. https://doi.org/10.1172/JCI141513.

Horing, M., et al., 2021. Accurate quantification of lipid species affected by isobaric overlap in Fourier-transform mass spectrometry. J. Lipid Res., 100050 https://doi.org/10.1016/j.jlr.2021.100050.

Hu, J., et al., 2020. Fibrinogen-like protein 2 aggravates nonalcoholic steatohepatitis via interaction with TLR4, eliciting inflammation in macrophages and inducing hepatic lipid metabolism disorder. Theranostics 10, 9702–9720. https://doi.org/10.7150/thno.44297.

Ioannou, G.N., et al., 2022. Pcsk9 deletion promotes murine nonalcoholic steatohepatitis and hepatic carcinogenesis: role of cholesterol. Hepatol. Commun. 6, 780–794. https://doi.org/10.1002/hep4.1858.

Jamialahmadi, T., et al., 2022. Impact of bariatric surgery on circulating PCSK9 levels as a marker of cardiovascular disease risk: a meta-analysis. Arch. Med. Sci. 18, 1372–1377. https://doi.org/10.5114/aoms/152685.

Jensen, M.D., 2008. Role of body fat distribution and the metabolic complications of obesity. J. Clin. Endocrinol. Metab. 93, S57–S63.
Kotowski, I.K., et al., 2006. A spectrum of PCSK9 alleles contributes to plasma levels of low-density lipoprotein cholesterol. Am. J. Hum. Genet. 78, 410–422. https://doi.org/10.1086/500615.
Krautbauer, S., et al., 2016. Relevance in the use of appropriate internal standards for accurate quantification using LC-MS/MS: tauro-conjugated bile acids as an example. Anal. Chem. 88, 10957–10961. https://doi.org/10.1021/acs.analchem.6b02596.
Lebeau, P.F., et al., 2019a. Pcsk9 knockout exacerbates diet-induced non-alcoholic steatohepatitis, fibrosis and liver injury in mice. JHEP Rep. 1, 418–429. https://doi.org/10.1016/j.jhepr.2019.10.009.
Lebeau, P.F., et al., 2019b. Diet-induced hepatic steatosis abrogates cell-surface LDLR by inducing de novo PCSK9 expression in mice. J. Biol. Chem. 294, 9037–9047. https://doi.org/10.1074/jbc.RA119.008094.
Lebeau, P.F., et al., 2021. The loss-of-function PCSK9Q152H variant increases ER chaperones GRP78 and GRP94 and protects against liver injury. J. Clin. Invest. 131. https://doi.org/10.1172/JCI128650.
Liebisch, G., et al., 2004. High-throughput quantification of phosphatidylcholine and sphingomyelin by electrospray ionization tandem mass spectrometry coupled with isotope correction algorithm. Biochim. Biophys. Acta 1686, 108–117. https://doi.org/10.1016/j.bbalip.2004.09.003.
Liebisch, G., et al., 2006. High throughput quantification of cholesterol and cholesteryl ester by electrospray ionization tandem mass spectrometry (ESI-MS/MS). Biochim. Biophys. Acta 1761, 121–128. https://doi.org/10.1016/j.bbalip.2005.12.007.
Luquero, A., et al., 2022. Differential cholesterol uptake in liver cells: a role for PCSK9. FASEB J. 36, e22291. https://doi.org/10.1096/fj.202101660RR.
Marengo, A., et al., 2015. Liver cancer: connections with obesity, fatty liver, and cirrhosis. Annu. Rev. Med. 67, 103–117. https://doi.org/10.1146/annurev-med-090514-013832.
Masternak, M.M., et al., 2012. Metabolic effects of intra-abdominal fat in GHRKO mice. Aging Cell 11, 73–81. https://doi.org/10.1111/j.1474-9726.2011.00763.x.
Mc Auley, M.T., 2020. Effects of obesity on cholesterol metabolism and its implications for healthy ageing. Nutr. Res. Rev. 33, 121–133. https://doi.org/10.1017/S0954422419000258.
Mijiti, T., et al., 2024. Inhibition of hepatic PCSK9 as a novel therapeutic target ameliorates metabolic steatohepatitis in mice. Int. Immunopharmacol. 143, 113621. https://doi.org/10.1016/j.intimp.2024.113621.
Mulder, P., et al., 2016. Surgical removal of inflamed epididymal white adipose tissue attenuates the development of non-alcoholic steatohepatitis in obesity. Int. J. Obes. (Lond) 40, 675–684. https://doi.org/10.1038/ijo.2015.226.
Nabi, O., et al., 2022. Comorbidities are associated with fibrosis in NAFLD subjects: a nationwide study (NASH-CO study). Dig. Dis. Sci. 67, 2584–2593. https://doi.org/10.1007/s10620-021-07032-z.
Nguyen, A., et al., 2016. Stromal vascular fraction: a regenerative reality? Part 1: current concepts and review of the literature. J. Plast. Reconstr. Aesthet. Surg. 69, 170–179. https://doi.org/10.1016/j.bjps.2015.10.015.
Paquette, M., et al., 2020. Circulating PCSK9 is associated with liver biomarkers and hepatic steatosis. Clin. Biochem. 77, 20–25. https://doi.org/10.1016/j.clinbiochem.2020.01.003.
Rein-Fischboeck, L., et al., 2017. Tubulin alpha 8 is expressed in hepatic stellate cells and is induced in transformed hepatocytes. Mol. Cell. Biochem. 428, 161–170. https://doi.org/10.1007/s11010-016-2926-4.
Rein-Fischboeck, L., et al., 2019. Variations in hepatic lipid species of age-matched male mice fed a methionine-choline-deficient diet and housed in different animal facilities. Lipids Health Dis. 18, 172. https://doi.org/10.1186/s12944-019-1114-4.
Rimbert, A., et al., 2021. Genetic inhibition of PCSK9 and liver function. JAMA Cardiol. 6, 353–354. https://doi.org/10.1001/jamacardio.2020.5341.
Roubtsova, A., et al., 2011. Circulating proprotein convertase subtilisin/kexin 9 (PCSK9) regulates VLDLR protein and triglyceride accumulation in visceral adipose tissue. Arterioscler. Thromb. Vasc. Biol. 31, 785–791. https://doi.org/10.1161/ATVBAHA.110.220988.
Ruscica, M., et al., 2016. Liver fat accumulation is associated with circulating PCSK9. Ann. Med. 48, 384–391. https://doi.org/10.1080/07853890.2016.1188328.
Sarvari, A.K., et al., 2021. Plasticity of epididymal adipose tissue in response to diet-induced obesity at single-nucleus resolution. Cell Metab. 33, 437–453 e5. https://doi.org/10.1016/j.cmet.2020.12.004.
Schaffler, A., et al., 2005. Mechanisms of disease: adipocytokines and visceral adipose tissue–emerging role in intestinal and mesenteric diseases. Nat. Clin. Pract. Gastroenterol. Hepatol. 2, 103–111.
Schattenberg, J.M., Galle, P.R., 2010. Animal models of non-alcoholic steatohepatitis: of mice and man. Dig. Dis. 28, 247–254. https://doi.org/10.1159/000282097.
Scherer, M., et al., 2009. Rapid quantification of bile acids and their conjugates in serum by liquid chromatography-tandem mass spectrometry. J. Chromatogr. B Analyt. Technol. Biomed. Life Sci. 877, 3920–3925. https://doi.org/10.1016/j.jchromb.2009.09.038.
Schott, H.F., et al., 2018. A validated, fast method for quantification of sterols and gut microbiome derived 5alpha/beta-stanols in human feces by isotope dilution LC-high-resolution MS. Anal. Chem. 90, 8487–8494. https://doi.org/10.1021/acs.analchem.8b01278.
Scicali, R., et al., 2021. Analysis of steatosis biomarkers and inflammatory profile after adding on PCSK9 inhibitor treatment in familial hypercholesterolemia subjects with nonalcoholic fatty liver disease: a single lipid center real-world experience. Nutr. Metab. Cardiovasc. Dis. 31, 869–879. https://doi.org/10.1016/j.numecd.2020.11.009.
Shafiq, M., et al., 2020. Effects of proprotein convertase subtilisin/kexin type-9 inhibitors on fatty liver. World J. Hepatol. 12, 1258–1266. https://doi.org/10.4254/wjh.v12.i12.1258.
Spirk, M., et al., 2020. Chemerin-156 is the active isoform in human hepatic stellate cells. Int. J. Mol. Sci. 21. https://doi.org/10.3390/ijms21207555.
Stenman, L.K., et al., 2012. High-fat-induced intestinal permeability dysfunction associated with altered fecal bile acids. World J. Gastroenterol. 18, 923–929. https://doi.org/10.3748/wjg.v18.i9.923.
Takahashi, M., et al., 2008. Chemerin enhances insulin signaling and potentiates insulin-stimulated glucose uptake in 3T3-L1 adipocytes. FEBS Lett. 582, 573–578.
Temple, K.A., et al., 2007. Uncoupling of 3T3-L1 gene expression from lipid accumulation during adipogenesis. FEBS Lett. 581, 469–474. https://doi.org/10.1016/j.febslet.2007.01.007.
Theocharidou, E., et al., 2018. The role of PCSK9 in the pathogenesis of non-alcoholic fatty liver disease and the effect of PCSK9 inhibitors. Curr. Pharm. Des. 24, 3654–3657. https://doi.org/10.2174/1381612824666181010123127.
Thorlacius-Ussing, G., et al., 2016. Interleukin-1β regulates PCSK9 and LDL receptor expression together with de novo cholesterol synthesis in HepG2 cells. Glob. J. Gastroenterol. Hepatol. 4, 36–44.
Tilg, H., 2010. The role of cytokines in non-alcoholic fatty liver disease. Dig. Dis. 28, 179–185. https://doi.org/10.1159/000282083.
Tilg, H., Moschen, A., 2010. Weight loss: cornerstone in the treatment of non-alcoholic fatty liver disease. Minerva Gastroenterol. Dietol. 56, 159–167.
Uchida, A., et al., 2012. Reduced triglyceride secretion in response to an acute dietary fat challenge in obese compared to lean mice. Front. Physiol. 3, 26. https://doi.org/10.3389/fphys.2012.00026.
Wajchenberg, B.L., 2000. Subcutaneous and visceral adipose tissue: their relation to the metabolic syndrome. Endocr. Rev. 21, 697–738.
Wanninger, J., et al., 2012. Adiponectin upregulates hepatocyte CMKLR1 which is reduced in human fatty liver. Mol. Cell. Endocrinol. 349, 248–254. https://doi.org/10.1016/j.mce.2011.10.032.
Wargny, M., et al., 2018. Circulating PCSK9 levels are not associated with the severity of hepatic steatosis and NASH in a high-risk population. Atherosclerosis 278, 82–90. https://doi.org/10.1016/j.atherosclerosis.2018.09.008.
Weber, F., et al., 2023. Expression and function of BMP and activin membrane-bound inhibitor (BAMBI) in chronic liver diseases and hepatocellular carcinoma. Int. J. Mol. Sci. 24. https://doi.org/10.3390/ijms24043473.
Xia, X.D., et al., 2021. Regulation of PCSK9 expression and function: mechanisms and therapeutic implications. Front. Cardiovasc. Med. 8, 764038. https://doi.org/10.3389/fcvm.2021.764038.
Xu, L., et al., 2023. Zhuyu pill alleviates nonalcoholic fatty liver disease by regulating bile acid metabolism through the gut-liver Axis. ACS Omega 8, 29033–29045. https://doi.org/10.1021/acsomega.3c01955.
Yeh, M.M., Brunt, E.M., 2014. Pathological features of fatty liver disease. Gastroenterology 147, 754–764. https://doi.org/10.1053/j.gastro.2014.07.056.
Younossi, Z., et al., 2018. Global burden of NAFLD and NASH: trends, predictions, risk factors and prevention. Nat. Rev. Gastroenterol. Hepatol. 15, 11–20. https://doi.org/10.1038/nrgastro.2017.109.
Zaid, A., et al., 2008. Proprotein convertase subtilisin/kexin type 9 (PCSK9): hepatocyte-specific low-density lipoprotein receptor degradation and critical role in mouse liver regeneration. Hepatology 48, 646–654. https://doi.org/10.1002/hep.22354.
Zeng, H., et al., 2022. Changes in the fecal metabolome accompany an increase in aberrant crypt foci in the colon of C57BL/6 mice fed with a high-fat diet. Biomedicines 10. https://doi.org/10.3390/biomedicines10112891.
Zenti, M.G., et al., 2020. Impact of bariatric surgery-induced weight loss on circulating PCSK9 levels in obese patients. Nutr. Metab. Cardiovasc. Dis. 30, 2372–2378. https://doi.org/10.1016/j.numecd.2020.07.013.